

UC Office of the President

Journal Articles

Title

Impact of Debris Removal Post-Wildfires on Pavement Fatigue and Rutting Lives: Case Studies of California's Camp and Carr Fires

Permalink

<https://escholarship.org/uc/item/8hx274h3>

Authors

Zarei, Ali

Kim, Changmo

Butt, Ali Azhar

et al.

Publication Date

2024-10-23

DOI

10.1177/03611981241283458

Peer reviewed

Impact of Debris Removal Post-Wildfires on Pavement Fatigue and Rutting Lives: Case Studies of California's Camp and Carr Fires

Transportation Research Record
1–17

© The Author(s) 2024



Article reuse guidelines:

sagepub.com/journals-permissions

DOI: 10.1177/03611981241283458

journals.sagepub.com/home/trr

Ali Zarei¹ , Changmo Kim¹ , Ali Azhar Butt¹ , Rongzong Wu¹ ,
Jeremy David Lea¹ , Jessica Erdahl², and Somayeh Nassiri¹ 

Abstract

Between 2017 and 2018, California experienced a series of four devastating fires, including the Camp and Carr Fires, which ranked among the most destructive fires in U.S. history. During these fires, roads were critical in the evacuation, rescue operations, goods transportation, and access to critical services. Additionally, postfire, road infrastructure became crucial for removing hazardous and nonhazardous waste from fire-affected areas to major landfills and recycling facilities. Despite the significance of pavements in this process, previous studies have not quantitatively assessed the potential damage caused to pavements by the additional trucks used in debris removal operations. This research aimed to address this knowledge gap by collecting precise traffic data for the routes taken to waste management facilities, including data on the number of trips involved in debris transportation. The traffic information was then utilized to calculate changes in equivalent single axle loads and traffic index values for pavement design. Pavement structures were obtained from the available core database. Pavement simulation results showed that of the nine studied highways, only one exhibited a reduction in cracking life of about 2 years. However, Skyway, the main artery in the town of Paradise, demonstrated a significantly accelerated fatigue cracking failure by 14.3 years. A sensitivity analysis of fire intensity showed other highway sections that were structurally adequate could be affected by larger fires. The presented methodology could be used in traffic planning as part of debris management operations to avoid vulnerable pavement sections.

Keywords

infrastructure, pavements, resilience, disaster response, recovery, disaster recovery

The combined impacts of global climate change and human development in the wildland–urban interface have heightened the risk of catastrophic wildfires in many regions worldwide, including approximately one-third of the United State's population (1, 2). California, in particular, witnessed a string of four devastating fires over 14 months in 2017 and 2018, which rank among the most destructive in the history of the United States (3).

Transportation infrastructure is vital during fire events in facilitating evacuation, rescue operations, goods transportation, and access to critical services (4). Although asphalt pavements are not prone to direct burning during fires, as the asphalt binder requires temperatures around 900°F to ignite (5), ignition can occur

if trees, vegetation, oil, or vehicles catch fire on the pavement surface. In such cases, the damage is generally confined to the area of the abandoned burning object, leading to localized surface scarring and destruction. However, widespread damage can result from the intense heat in wildfire-stricken areas, causing the asphalt to soften and deform or crack under the weight of heavy

¹Department of Civil and Environmental Engineering, University of California Pavement Research Center, UC Davis, Davis, CA

²Public Works Department, Engineering, Town of Paradise

Corresponding Author:

Somayeh Nassiri, nassiri@ucdavis.edu

fire trucks and emergency traffic (6). Similarly, on rigid pavements, burning objects may damage the pavement at the location as concrete loses mechanical properties resulting from the loss of bound water, decomposition of calcium hydroxide, and disassociation of calcium carbonates at various temperature ranges (7, 8). These types of immediate damage to construction materials during an active fire from high temperatures, especially to concrete foundations, structures, and pavements in tunnels, have been discussed extensively in the literature (9). Literature is also abundant on potential post-fire hazards, such as landslides, mudslides, and other consequences (10).

However, notwithstanding the immediate impact of high temperatures on asphalt and concrete, pavements play a critical role in postfire recovery. Pavements facilitate the removal and transportation of various types of waste from fire-affected areas to major landfill-, construction-, and demolition recycling facilities. These materials include demolition waste, hazardous ash, soil, dead trees and vegetation, mixed metals, charred wood, automobiles, and other debris (11, 12). However, the pavement damage caused by debris removal operations has not been studied before. Wildfires pose significant social, economic, and physical impacts on transportation infrastructure and necessitate special provisions and planning for departments of transportation' (DOTs') financial, operational, and maintenance schedules and budget allocations. This is partly because of resource constraints, as DOTs may not have the necessary resources to properly analyze the physical impact of fire events on pavements and other transportation assets (13).

This study aimed to address this knowledge gap by collecting accurate data on the truckloads and number of trips involved in debris transportation following two major wildfires in California. Subsequently, pavement simulations were conducted to analyze the actual routes taken by the trucks to transport the debris to landfills and recycling facilities to determine any potential fatigue and rutting life-shortening. The presented case studies provide valuable insights into the actual physical impact and include hypothetical worst-case scenarios as an example of how the potential extent of future events to the physical road network can be estimated.

Understanding and quantifying the damage caused by fires to the pavement structure helps DOTs and local governments prioritize and allocate resources to address the vulnerable transportation infrastructure during high-risk wildfires and other climate-related hazards. By addressing the potential impacts of postfire transportation on the road network, agencies can ensure the continued functionality, safety, and resilience of the transportation system, even in the aftermath of wildfires.

Case Studies of California's 2018 Camp Fire and Carr Fire

Description

Camp Fire: Butte County. Threatened by 13 fires in Northern California since 1999, the town of Paradise is at high risk of wildfire (14). The Camp Fire incident in November 2018 burned 153,336 acres, killed 86 people, injured three others, and destroyed 18,804 structures, equivalent to 95% of homes and businesses in the Town of Paradise. Around \$12.5 billion in insured losses were reported, making this fire the costliest disaster worldwide in 2018 (15, 16). The aerial photos of Paradise before and after the fire, as shown in Figure 1, illustrate the extent of the damage.

The disaster recovery included the removal of over 3.6 million tons of waste and used a significant amount of resources as Camp Fire created the largest hazardous material cleanup operation in the United States' history (14). The debris consisted of 2.24 million tons of burned debris and ash, 710,000 tons of recycled concrete, 680,000 tons of contaminated soil and ash, and 52,000 tons of recycled metal, resulting in 600,000 total trips, according to the report published by the California Department of Resources Recycling and Recovery (CalRecycle) (17) as well as dead trees and vegetation.

Two pavement damage categories were identified in the damage assessment forms (DAFs) obtained from Paradise: pavement scarring resulting from abandoned burning vehicles and postfire heavy truck traffic damage from 3.7 million tons of debris removal. Pavement condition surveys in January 2019 (after the fire incident, pre-debris removal) and September 2019 (8 months after the fire incident, post-debris removal) were conducted by the town. These surveys provided insights into the immediate impact of the fire on the pavement and the subsequent damage caused by the heavy truck traffic involved in debris hauling. The survey results and four pavement performance metrics are summarized in Table 1.

Based on the DAFs and the summary in Table 1, it was found that longitudinal and transverse cracks had extended and interconnected, forming alligator cracks, which indicated pavement failure over the 8 months as a result of water infiltration and heavy truck loads. Significant rutting was observed throughout the roadway network, especially in segments where trucks frequently stopped and started.

Figure 2a shows local scarring damage from a burned vehicle, and Figure 2b shows rutting and fatigue cracking damage to Skyway, the main artery of Paradise City, after debris removal operations.

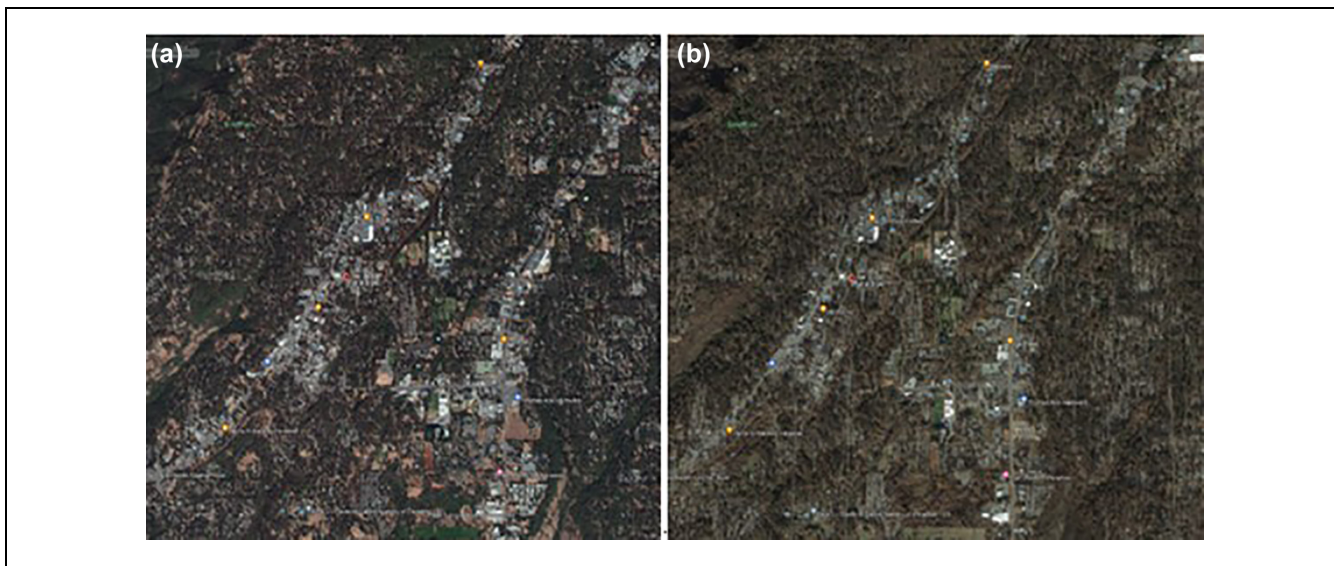


Figure 1. Town of Paradise (a) before Camp Fire (September 2018) and (b) after Camp Fire (December 2018).

Source: Google Maps™.

Table 1. Pavement Condition Surveys in January 2019 (After the Fire Incident, Predebris Removal) and September 2019 (8 Months After the Fire Incident, Postdebris Removal)

Performance metric	January condition	September condition	Pavement deterioration occurred: Yes or No
Cracking	Moderate/good	Moderate	Yes: increase in cracking
Roughness	Moderate/good	Moderate	No: minimal increase in deterioration
Rutting	Moderate	Moderate/poor	Yes: isolated deterioration, especially in areas where truck traffic repeatedly starts and stops
Texture	Moderate	Poor	Yes: major deterioration



Figure 2. Town of Paradise: (a) local scarring damage from burning cars and (b) fatigue and rutting of Skyway in Paradise City.

Carr Fire: Shasta County and Trinity County. The Carr Fire incident occurred on July 23, 2018, from a spark produced from the wheel rim of a vehicle with a flat tire

(18), which resulted in the burning of 229,651 acres of fields, killing seven people, and destroying 1,614 residential and commercial structures (19) and causing more

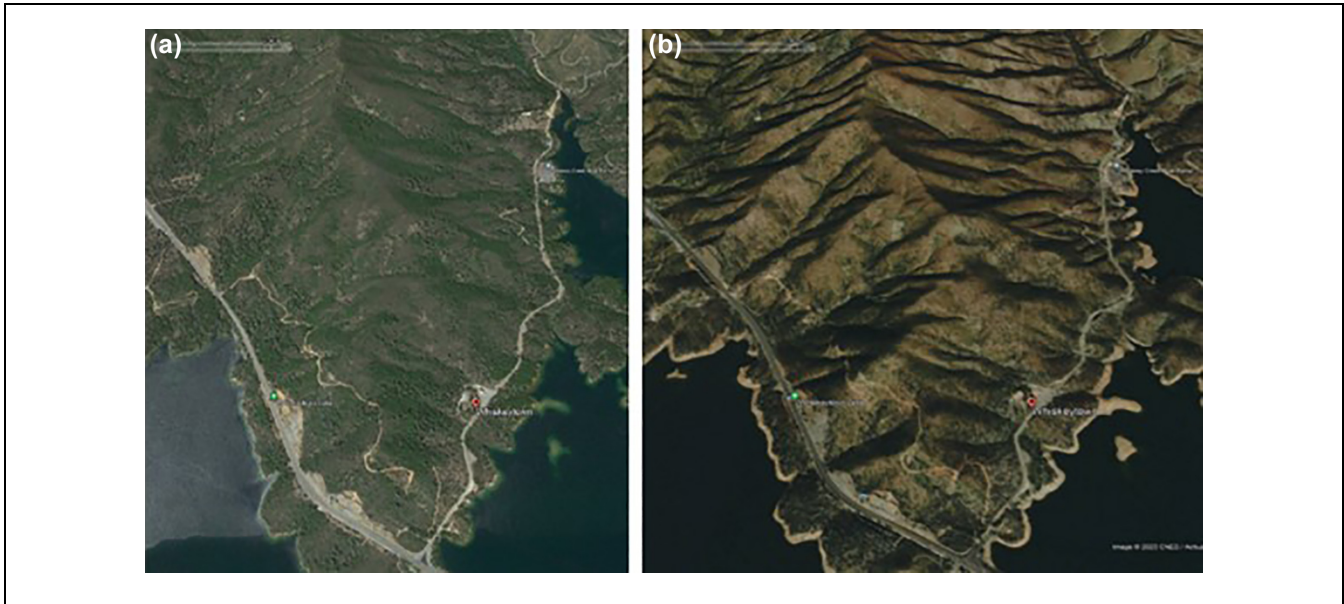


Figure 3. Fire-stricken area (a) before the Carr wildfire (June 2018) and (b) after the Carr wildfire (February 2020)
Source: Google Maps™.

than \$1.6 billion in damages (20). Carr Fire, at the time of writing, is considered to be the seventh-largest and sixth-most destructive fire in the history of California (18). Unlike Camp Fire, where undamaged structures were comprehensively recorded in postfire damage inspection reports by Cal Fire (California Department of Forestry and Fire Protection), only aerial imagery was used for Carr Fire (21). Around 521,619 tons of debris were removed, and 46,807 truckloads were reported. The debris included metals, ash (soil and debris), soil, and concrete (22).

Photos taken from Google Maps of the fire-stricken area before and after Carr Fire are shown in Figure 3, *a* and *b*.

Method

Truck Traffic Counts and Loads. According to the Camp Fire Debris Removal Operation Traffic Management Plan report (23), seven facilities received 3.66 million tons of wildfire debris, including metals, debris ashes, soil scrap, concrete, and asbestos, from the Camp Fire-stricken sites. The total debris was hauled by 309,239 truck trips from the fire sites to the facilities between February and August 2019. Table 2 shows the road routes taken by the hauling trucks, the total load, and the number of truck trips to each facility during the debris removal activities.

Baseline Truck Traffic and Extra Truck Traffic Volumes. The study only included traffic analysis for debris removal postdisaster. Any traffic surge from fire suppression and

rescue activities during the active fire event was not included in the study. The baseline truck traffic information for the selected highway sections was acquired from the Traffic Census Program, annually updated by the California Department of Transportation (Caltrans) (24). The baseline truck traffic information includes each section's annual daily traffic and truck percentages by axle type (i.e., two-, three-, four-, and five-axes). The additional truck traffic volumes caused by removing wildfire debris were added to the 2019 baseline truck traffic volumes for the corresponding highway sections.

This study focused on the highway sections to compare the performance of asphalt pavement with two scenarios (i.e., the baseline scenarios without and those with wildfire truck traffic) for 20 years of pavement service life. In the two scenarios, equivalent single axle loads (ESALs) and traffic index (TI) values were calculated, and the corresponding axle load spectra were chosen from the Caltrans pavement management system (PaveM) (Table 3) (24, 25). TIs of the scenarios with wildfire were slightly higher than the baseline scenario owing to the truck trips to remove the wildfire debris in 2019. Interstate 5 (I-5) sections showed a slight difference (0.02 for northbound [NB] and 0.03 for southbound [SB]) because the truck traffic without the debris removal trucks was already high, with a TI at around 14 for a 20-year design life. However, Skyway in the town of Paradise showed the largest increase in TI from 8.0 without- and 9.53 with wildfire trucks.

Five axle load spectra developed in a previous study based on Caltrans' weigh-in-motion data (24, 26) were

Table 2. Main Routes, Truck Load, and Number of Trips to each Facility (23)

Waste management destination	Main routes of the debris removal trucks	Load (ton)	No. of trips
Camp Fire			
Recology Ostrom Road Landfill	Highway 191 southbound (Paradise), Highway 70 southbound (north of Orville), Highway 65 southbound (Junction 70)	1,552,522	113,107
Waste Management Anderson Landfill	Highway 99 northbound (Chico), Highway 5 northbound (Red Bluff), West Anderson Road	718,523	56,519
Butte County Neal Road Landfill	Neal Road (Paradise)	629,830	46,817
Granite Pacific Heights Recycling Facility	Highway 191 southbound (Paradise), Highway 70 southbound (north of Orville)	451,097	39,133
Franklin Neal Road Recycling Facility	Neal Road (Paradise)	256,007	20,957
Odin Metal Processing Facility	Highway 191 southbound (Paradise), Highway 70 southbound (north of Orville)	51,915	32,695
Crown Metals Recycling Facility	Highway 191 southbound (Paradise), Highway 70 southbound (north of Orville)	22	11
Total		3,659,916	309,239
Carr Fire			
Waste Management Anderson Landfill	Highway 5 southbound, West Anderson Road	411,540	37,413
Crystal Creek Aggregate	Highway 299 southbound near Shasta	54,809	4,983
Troy Leckey Land Clearing	Highway 299 southbound near Shasta	25,889	2,354
West Central Landfill	Swasey Drive, Placer Road	17,280	1,571
Steel Mill Recycling	Not identified	7,136	649
J.F. Shea Construction	Highway 5 southbound,	4,965	451
Total		521,619	47,420

assigned to each state pavement section. Spectrum 1 denotes the lightest axle load, and Spectra 5 is the heaviest. A preliminary case study was undertaken for Highway 99 NB Butte County (BUT) postmile (PM) 32 to 43 to determine the effect of temporal modifications to Caltrans' existing load axle spectra to reflect the changes in axle loads during the exact time of debris removal. The results of the preliminary study showed the changes were negligible. The most significant change in the number of axles was approximately 9% in June 2019. The average change in the number of axles was 4% for the 7-month active debris haul period. This change in axle load spectra for the 7 months over the 20-year analysis period was not significant enough to make a noticeable difference with or without wildfire debris haul truck trips. More details about this preliminary study can be found in the project report (27). Based on the preliminary study's findings, the existing axle load spectra were used, and other traffic parameters (including traffic volumes, ESALs, and TI) were adjusted for the added debris truck traffic, as discussed below.

The assigned axle load spectra for each pavement section were as follows: I-5 northbound in Tehama County (TEH) PM 28 to 41, which served the debris removal trucks after Camp Fire, had Spectra 4, which is the second heaviest axle load spectra. I-5 southbound in Shasta County (SHA), PM 4 to 19, which served the debris

removal trucks after Carr Fire had Spectra 3, the medium axle load spectra. I-5 functions as the longitudinal freight corridor in California. State Highway 99 sections in BUT, PM 32 to 43, and TEH, PM 0 to 24, had Spectra 3 according to Caltrans' PaveM (25).

The traffic data, including traffic volumes, ESALs, and TIs used for simulations, are shown in Table 3. The changes in TI from debris trucks from Camp Fire ranged between 0.02 for I-5 northbound (TEH 28–41) and 1.53 for Skyway in the town of Paradise. Route 191 SB (BUT 0–10) and 70 eastbound (EB) (BUT 0–20) had the highest number of debris truck trips, resulting in the highest added ESALs and a high TI change of 1.12 and 0.23, respectively. Skyway, which carried most of the debris trucks out of the town of Paradise, had a significant change in TI from 8 to 9.53. The total amount of debris and consequently loaded truck trips was much less for the Carr Fire, resulting in an added TI of only 0.04 for 299 EB (SHA 19–23) and 0.02 for I-5 southbound (SHA 4–19).

The approach used here distributes the debris truck traffic over the design life, which means the damage development is also spread out over this period rather than appearing immediately after the debris haul event. Although this method does not accurately reflect the exact timing of damage development, it effectively represents the cumulative damage that occurs over the design life.

Table 3. Traffic Data of the Selected Section for CalME Simulations

Road section (county, postmiles)	Traffic volume (two-way)					20-year ESAL			Calculated TI		
	Trucks	2 axles	3 axles	4 axles	5 + axles	ESAL Without fire	ESAL from fire	Total ESAL	Without fire	With wildfire	WIM spectra
Camp Fire											
99 NB (BUT, 32-43)	5,906	4,245	288	123	1,250	27,919,880	570,400	28,490,280	13.38	13.41	3
99 NB (tEh, 0-24)	1,764	589	96	31	1,048	7,894,910	570,400	8,465,310	11.51	11.61	3
5 NB (TEH, 28-41)	7,197	769	281	114	6,033	42,950,180	570,400	43,520,580	14.09	14.11	4
191 SB (BUT, 0-10)	424	160	126	34	103	1,151,870	1,876,800	3,028,670	9.15	10.27	1
70 EB (BUT, 0-20)	3,095	1,179	393	202	1,321	11,232,200	1,876,800	13,109,000	12.00	12.23	2
70 EB (YUB, 8-25)	2,703	612	555	178	1,358	11,323,420	1,140,800	12,464,220	12.02	12.15	2
65 SB (YUB, 4-9)	4,827	2,075	1,012	506	1,234	13,283,730	1,140,800	14,424,530	12.25	12.37	1
Skyway in the town of Paradise	NA	NA	NA	NA	NA	371,661	1,251,200	1,622,861	8.00	9.53	na
Carr Fire											
299 EB (SHA, 19-23)	890	552	94	11	233	2,191,550	80,960	2,272,510	9.88	9.92	3
5 SB (SHA, 4-19)	4,225	1,011	181	47	2,986	38,235,350	415,840	38,651,190	13.89	13.91	3

Note: NA = not available; na = not applicable; CalME = mechanistic pavement design software; ESAL = equivalent single axle load; TI = traffic index; BUT = Butte County; the = Tehama County; SHA = Shasta County; YUB = Yuba County; WIM = weigh-in-motion; NB = northbound; SB = southbound; EB = eastbound.

Pavement Structural Simulations

CalME v3.0, mechanistic pavement design software, jointly developed by Caltrans and the University of California Pavement Research Center, was used for the pavement simulations. CalME uses an incremental-recursive damage process. In the model for fatigue damage of asphalt layers, for example, the strain, the modulus, and the temperature may change from increment to increment. Therefore, the first step in the process is to calculate the effective number of load applications that would have been required with the present parameters to produce the condition at the beginning of the increment. In the second step, the new condition, at the end of the increment, is calculated for the effective number of load applications plus the number of applications during the increment. This process is repeated for each combination of axle type, load level, and the daily period during the increment. A load spectrum is used to distribute truck traffic into these combinations.

For asphalt permanent deformation (rutting), CalME uses a shear-based approach developed in an earlier study (28). Shear deformation is assumed to control rutting in asphalt. Rutting is computed using Equation 1. Inelastic or permanent strain in Equation 1 is derived from Equation 2, which is based on values of shear stress, τ , and elastic shear strain, γ^e , at a depth of 2 in. beneath the edge of the tire. The model also assumes rutting occurs solely in the top 4 in. of the hot mix asphalt (HMA) layer,

$$rd_{AC} = K \times \gamma^i \times h \quad (1)$$

where

rd_{AC} is vertical rutting depth in the asphalt concrete (AC),

γ^i is permanent (inelastic) shear strain at a 2-in. depth,

K is value relating permanent shear strain to rutting depth, and

h is thickness of the AC layer, with a maximum value of 4 in.

The permanent strain can be calculated from the gamma function shown in Equation 2,

$$\gamma^i = A \cdot \exp\left(\alpha \times \left[1 - \exp\left(-\ln(N)/\gamma\right) \times \left(1 + \ln(N)/\gamma\right)\right]\right) \times \gamma^e \quad (2)$$

where

γ^e is corresponding elastic shear strain,

N is effective number of load repetitions (i.e., number of load repetitions at the stress and strain level of the next time increment to reach the permanent shear strain calculated at the end of the current time increment), and

A , α , and γ are material-dependent model parameters.

Permanent deformation of unbound layers such as lightly cemented or unbound materials is based on the vertical resilient strain at the top of the layer, $\mu\varepsilon$, and stiffness of Layer E ,

$$d_p = A \times MN^\alpha \times \left(\frac{\mu\varepsilon}{\mu\varepsilon_{\text{ref}}}\right)^\beta \times \left(\frac{E}{E_{\text{ref}}}\right)^\gamma \quad (3)$$

where

d_p = permanent deformation in the layer,

MN = number of load applications in millions,

$\mu\varepsilon_{\text{ref}}$ = normalizing strain,

E_{ref} = normalizing stiffness, and

A , α , β , and γ are material-specific model parameters.

The CalME AC fatigue cracking model uses a multi-layer elastic program as the response submodel. In CalME, only traffic-related fatigue damage is considered. Details of the model can be found in other studies (29, 30). The key part of the model is Equation 4 for estimating fatigue life, MN_p ,

$$MN_p = A \times \left(\frac{\varepsilon}{\varepsilon_{\text{ref}}}\right)^\beta \times \left(\frac{E}{E_{\text{ref}}}\right)^{\beta/2} \quad (4)$$

where

ε is bending strain at the bottom of the asphalt layer, negative for tensile;

E is mix stiffness;

$\varepsilon_{\text{ref}} = -200$ microstrain (-200×10^{-6} in./in.), the reference bending strain;

$E_{\text{ref}} = 435$ kips per square inch, the reference stiffness; and

A and β are material-dependent model parameters.

Once the fatigue damage is determined, the percent of wheel path cracked, denoted as CRK, is assumed to relate to the fatigue damage through the following transfer function:

$$CRK = \frac{100}{1 + \left(\frac{\omega}{\omega_{50}}\right)^\beta} \quad (5)$$

where ω is the calculated fatigue damage, and ω_{50} and β are model parameters to be determined through field calibration. ω_{50} represents fatigue damage corresponding to 50% CRK, and it can be any value between 0 and 1.0. Each parameter might depend on additional factors such as pavement structure type, climate condition, and HMA layer thickness. The assumed transfer function represents an S-shaped curve that seems to match the observed cracking progression in the field. The mid-portion slope of the S-shaped curve is controlled by β . Accordingly, β is called the shape parameter, and it is always negative, with a higher absolute value suggesting a steeper ascent.

Table 4. Pavement Structure of Roads Used to Haul Debris to Waste Management Facilities

Name: highway number, direction (county, postmiles)	Time and PM of last treatment year (postmiles)	Pavement structure (ft)					
		RHMA	HMA	PCC	AB	CTB	ASB
Camp Fire							
99 NB (BUT 32–43)	2015 (PM30–37)	0.15	0.55	na	1.75	na	na
99 NB (TEH 0–24)	2012 (PM12–24)	na	0.90	0.50	na	na	na
5 NB (TEH 28–41)	2011 (no record after 2011)	na	0.85	na	1.65	na	na
191 SB (BUT 0–10)	2013 (PM0–11)	na	0.55	na	na	0.65	na
70 EB (BUT 0–20)	2014 (PM13–17)	na	0.75	na	0.50	na	0.75
70 EB (YUB 8–25)	2015 (PM 14–15)	na	0.75	na	1.00	na	na
65 SB (YUB 4–9)	2011 (no record after 2011)	0.15	0.55	na	0.50	na	na
Skyway in the town of Paradise	na	na	0.50	na	0.92	na	na
Carr Fire							
299 EB (SHA 19–23)	2012 (PM19–20)	na	0.90	na	0.40	na	na
5 SB (SHA 4–19)	2017 (PM4–6)	na	0.50	0.75	1.00	0.25	na

Note: na = not applicable; PM = postmile; BUT = Butte County; TEH = Tehama County; SHA = Shasta County; YUB = Yuba County; RHMA = rubberized hot mix asphalt; HMA = hot mix asphalt; PCC = Portland cement concrete; AB = aggregate base; CTB = cement-treated base; ASB = aggregate subbase.

Table 5. CalME Input Parameters used for all Simulated Sections

Parameter	Quantity	Parameter	Quantity
Traffic	As shown in Table 3	Binder type	Mix with PG 70–10
Climate zone	Inland Valley, California	Subgrade type	Silty sand
Simulation duration	20 years based on Caltrans' design practice	RHMA modulus-E (ksi)	722.0*
Vehicle speed	43.75 mph	HMA modulus-E (ksi)	1,230.6*
Simulation type	Deterministic: reliability = 50%	PCC modulus-E (ksi)	5076.3*
Rutting performance criteria	0.4 in.	AB modulus-E (ksi)	45.0*
Cracking performance criteria	10%	CTB modulus-E (ksi)	1508.1*
Structure	As shown in Table 4	ASB modulus-E (ksi)	35.0*

Note: RHMA = rubberized hot mix asphalt; HMA = hot mix asphalt; PCC = Portland cement concrete; AB = aggregate base; CTB = cement-treated base; ASB = aggregate subbase; ski = kips per square inch; PG = performance grade.

*These values represent the statewide medians of layer moduli used for routine pavement designs. For the HMA layer, the moduli are determined for 68°F and 10 Hz loading frequency.

Pavement Structures. The materials and pavement structures for CalME simulations were defined using the latest cross section of information based on extracted cores in the iGPR-Core database. iGPR illustrates the pavement structure profile by mapping the density of the structure layers with the data detected from a ground-penetrating radar (31). Time and PM treatments were extracted from PavEM (25), as shown in Table 4. Other information included in the table includes the route name, direction, county, PM, last treatment, and most updated structure of each pavement structure for both the Camp and Carr Fires. The subgrade soil type was unavailable for some sections but was characterized as sandy soil (SC) for those with available information. Therefore, SC was considered the subgrade type for all pavement sections. As seen in Table 2, most highway sections were HMA, varying between 0.5 and 0.9 ft. Two sections of 99 NB (BUT 32–43) and 65 SB (Yuba County [YUB] 4–9) had a 0.15-

ft rubberized hot mix asphalt overlay, and one was a Portland cement concrete (PCC) section. Almost all sections had an aggregate base (AB), except Highway 191 SB (BUT 0–10), which had a cement-treated base layer, and Highway 99 NB (TEH 0–24), which had a PCC layer. Only Highway 70 EB (BUT 0–20) had an aggregate subbase layer.

Table 4 also includes the structure of Skyway, the main route that was used to haul all the city debris from the Camp Fire out of Paradise City.

The CalME input parameters and their defined values for the pavement section are summarized in Table 5. The results are presented for rutting and cracking life in years. The performance criteria for rutting were set to 0.4 in. and 10% for cracking based on Caltrans' *Maintenance Manual*, Chapter A (32). The deterministic simulation for 20 years was used to predict median pavement life (i.e., with 50% reliability). The simulation start date for each

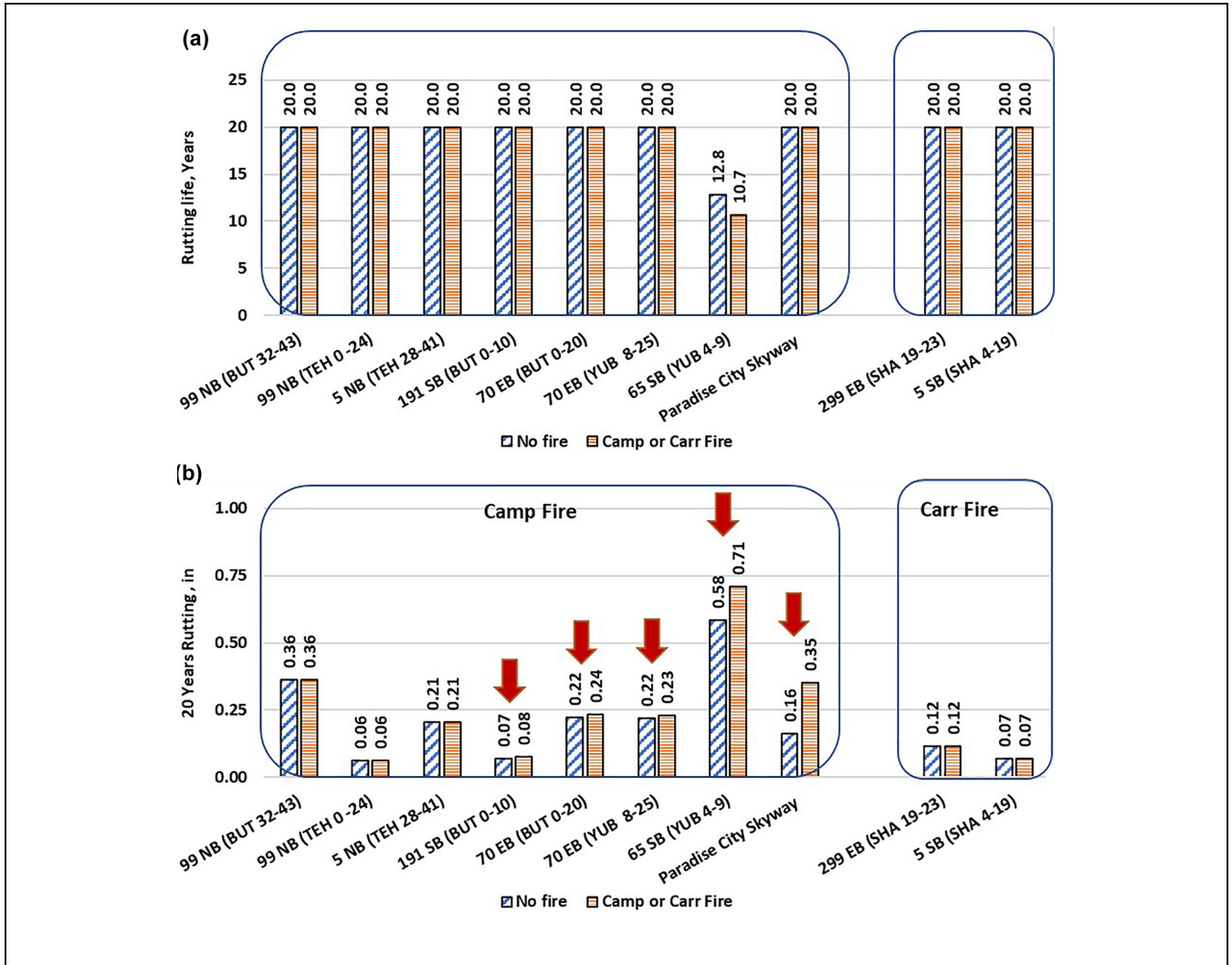


Figure 4. Impact of fire debris removal generated by Camp and Carr Fires on the rutting life of the pavements taken to waste management facilities: in (a) years and (b) 20-year rutting in inches.

pavement section was defined as the latest time of the last treatment presented in Table 5.

Results and Discussion

Impact of Fire Debris Truck Traffic

The outcomes of the CalME simulations are presented in Figure 4, *a* and *b*, for rutting life and the 20-year rutting amount, respectively, and in Figure 5 for fatigue cracking life for both the Camp and Carr Fires. In Figure 4*a*, a rutting life of 20 years illustrates a pavement that has passed the 0.4-in., 20-year rutting criteria. The pavements affected by the fire debris truck traffic are identified with a vertical down arrow on each graph.

As seen in Figure 4*a*, the structure of nearly all the simulated pavements was sufficient for rutting resistance for 20 years of existing truck traffic and the additional fire debris truck traffic. Similarly, it can be seen in Figure 4*b* that although debris trucks increased the 20-year rutting depth for some highways such as 191 SB (BUT 0–10), 70 EB (BUT 0–20), and 70 EB (YUB 8–25), the change was small and did not decrease the rutting lives of these sections. The only exception was 65 SB (YUB 4–9), which experienced rutting failure before the 20-year mark (Figure 4*a*). Without considering fire debris truck traffic, the rutting life of 65 SB (YUB 4–9) was 12.8 years for this section, which decreased by 2.1 years because of the trucks undertaking the Camp Fire debris removal. This premature failure was attributed to inadequate

HMA (0.55 ft) and AB (0.5 ft) thicknesses in this pavement section, which were insufficient to support the existing traffic loads of 13 million ESALs. The situation was then exacerbated by the added stress from the fire-related truckloads, which increased the TI from 12.25 to 12.37. It should be noted that the pavement simulations here were performed based on the last structural rehabilitation record available for this section, which was in 2011. If additional rehabilitation activities were performed on this section after 2011, the pavement simulation would have to be rerun to include a stronger structure. Skyway did not demonstrate a decrease in rutting life, based on the 0.4-in. failure criterion, according to Figure 4a. However, as seen in Figure 4b, 20-year rutting increased significantly and reached a value of 0.35 in. compared with 0.16 in. without the debris trucks. Rutting is visible in the field picture of Skyway taken after debris operations (Figure 2b).

Regarding Carr Fire, both simulated highways successfully accommodated the additional truckloads from fire debris removals without any rutting failure during the 20-year design life.

With respect to fatigue cracking, as seen in Figure 5a, the structures of five pavement sections were adequate to prevent fatigue cracking failure for 20 years despite the additional truck loads from Camp Fire. These five pavement sections showed zero cracking after 20 years, as seen in Figure 5b.

However, the structures of two highway sections were inadequate to pass the 20-year cracking criterion of 10%. These sections included 99 NB (BUT 32–43) and 65 SB (YUB 4–9). For 99 NB (BUT 32–43). Both sections had 100% cracking at the 20-year design life, as seen in Figure 5b. Fire debris truck traffic increased the TI of 65 SB (YUB 4–9) from 12.25 to 12.37, which reduced the cracking life of this section from the already low 10.3 years to 9.2 years. This reduction in cracking life for this section was commensurate with its rutting failure behavior discussed in the previous section.

In the case of Skyway, the TI increased from 8.0 to 9.53, resulting in a significant cracking life reduction of 14.1 years. As seen in Figure 5b, this street showed zero percent cracking without the debris trucks versus 100% cracking after debris operations. See pictures of this section in Figure 2b.

For the Carr Fire, Highway 299 EB (SHA 19–23) successfully accommodated the additional fire debris truckloads without any cracking failure during the 20-year design life. In contrast, Highway 5 SB (SHA 4–19) did not have sufficient structural capacity to resist cracking failure and showed a 100% 20-year cracking with or without considering the traffic from the Carr Fire. The TI change from debris removal was not large enough to induce any additional fatigue cracking.

The correlation between the asphalt layer thickness of the failed sections and their cracking life is shown in

Figure 5c. The strong correlation between the asphalt layer thickness and the cracking life ($R^2 = 0.98$) suggests that when considering debris truck traffic, the thickness of the asphalt layer plays a significant role. One conclusion is that vulnerable pavements could easily be identified as those that do not have sufficient structure to withstand their existing traffic and, if possible, should, therefore, be avoided by debris trucks during the planning stage. Another analysis shown in Figure 5d shows a strong correlation with a high coefficient of determination ($R^2 = 0.99$) between the reduction in cracking life and the increase in pavement TI. Again, this change in TI could be used as an indicative parameter, and limiting the values of the TI increase could be used during the debris traffic planning stage to avoid vulnerable pavements.

Assessment of Pavement Physical Conditions Based on Field Data

The field rutting, fatigue cracking (if any), and international roughness index (IRI) in years before and after fire debris truck traffic for three of the simulated segments was available from Caltrans' Pavement database and was used here to evaluate the overall physical conditions of the pavements and compare those with the simulation results, if possible. The three sections with available field data were 65 SB (YUB 4–9) and 299 EB (SHA 19–23) used for the Camp Fire debris cleanup and 99 NB (BUT 32–43) used for the Carr Fire cleanup.

Highway 65 (YUB 4–9) Before and After Camp Fire. Figure 6, a and b, shows the field rutting and IRI data for the NB and SB lanes of Highway 65 (YUB 4–9) in 2018, 2019, 2020, and 2021. Fatigue cracking was not recorded for those years. Given that the last structural/treatment record available for this section was for 2011, this section was 10 years old in 2021. Based on Figure 6a, 0.107 in. of rutting was reported for both directions. Figure 6b indicates an IRI of 71 in./mi in both directions, below the federal performance benchmark of 95 in./mi for a "Good" pavement ranking (33). Consequently, based on the rutting and IRI data, the pavement section appeared to be in an overall satisfactory condition at the midway point of its expected lifespan.

A comparison was made between the rutting and IRI of NB and SB lanes, aiming to determine the impact of debris removal traffic in 2019. With regard to rutting, SB, utilized by loaded debris trucks, exhibited a 29% increase from 2019 (pre-debris removal) to 2020 (post-debris removal). Conversely, NB rutting increased by 9% during the same period. This 20% differential rise in rutting between NB and SB suggests a potential

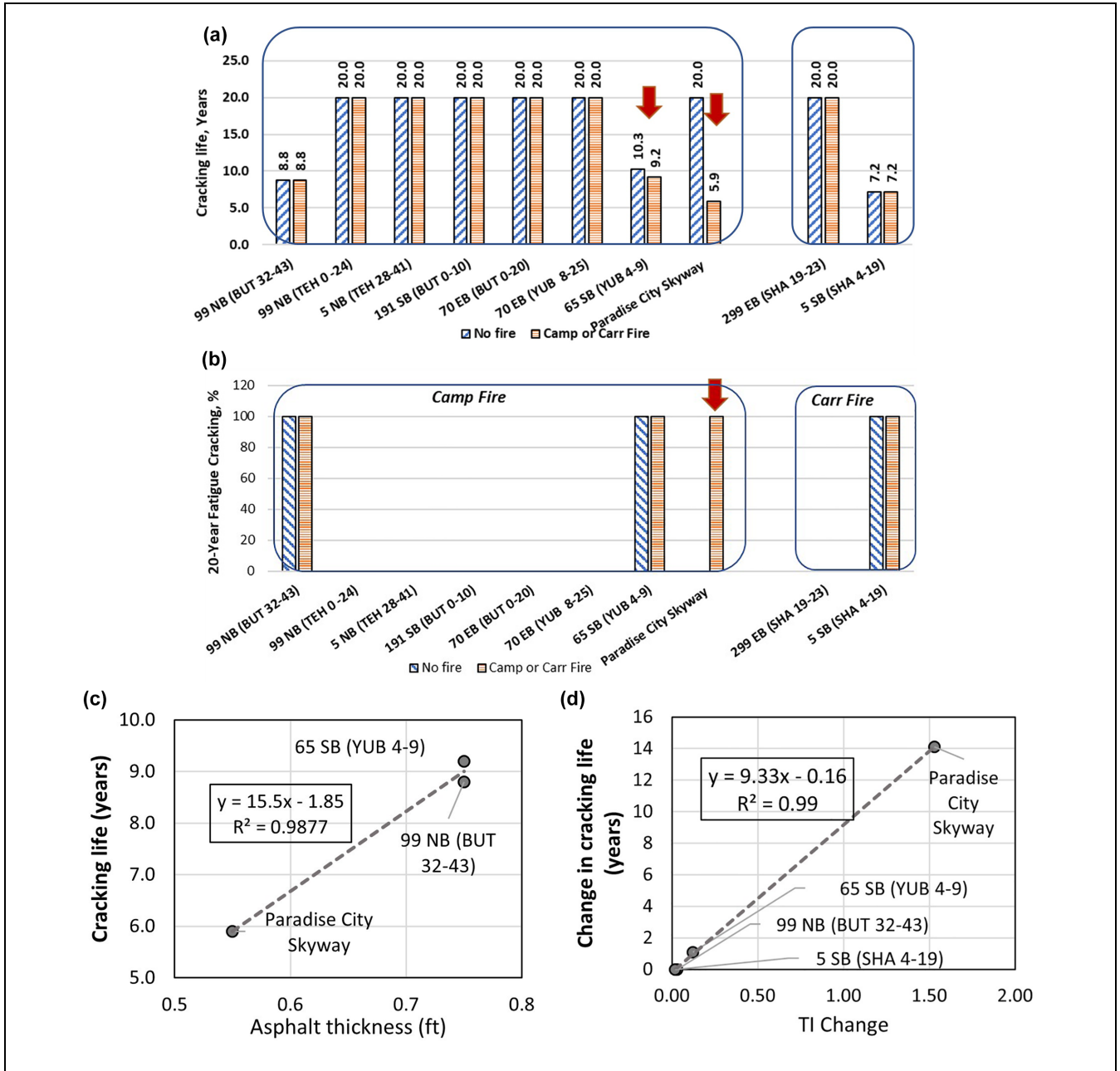


Figure 5. (a) Impact of fire debris removal generated by Camp and Carr Fires on the fatigue cracking life of the pavements taken to waste management facilities, (b) 20-year cracking in percentage, (c) correlation between asphalt layer thickness and cracking life of the pavement structures that failed within 20 years, and (d) the correlation between change in TI and change in the cracking life of the pavement structures that failed within 20 years.

influence of debris removal in 2019. However, this conclusion cannot be made with absolute certainty, given the possibility of other events resulting in a traffic spike in the SB direction of this section.

On the other hand, CalME simulations for this section displayed a more aggressive outlook than the actual performance, predicting a rutting failure of 0.4 in. at year 12.8 without debris trucks and 10.7 with debris truck

traffic. As seen in Figure 6b, SB IRI increased by 10%, whereas NB IRI increased by 3% from 2019 to 2020. Again, this accelerated IRI increase may be attributed to the loaded debris trucks utilizing the SB lane. Despite the structural simulations projecting a more rapid development of damage than observed in the field data, both simulations and field data converged on the possibility of damage resulting from debris trucks. It is important to

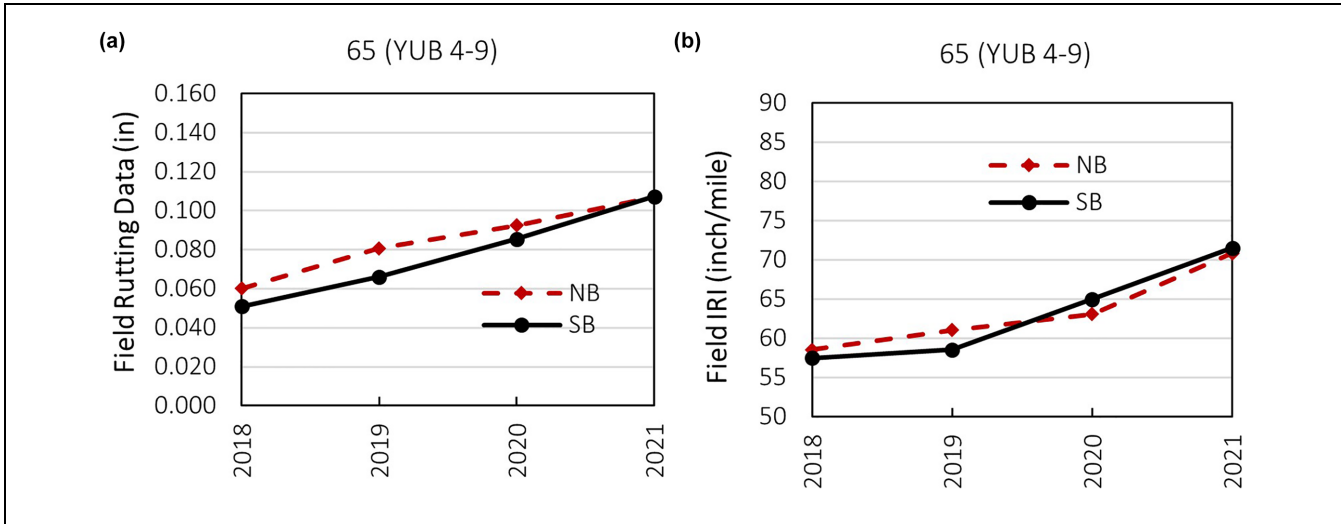


Figure 6. Field (a) rutting and (b) IRI data for 65 (YUB 4–9) NB and SB directions.
 Note: IRI = international rutting index; YUB = Yuba County; NB = northbound; SB = southbound.

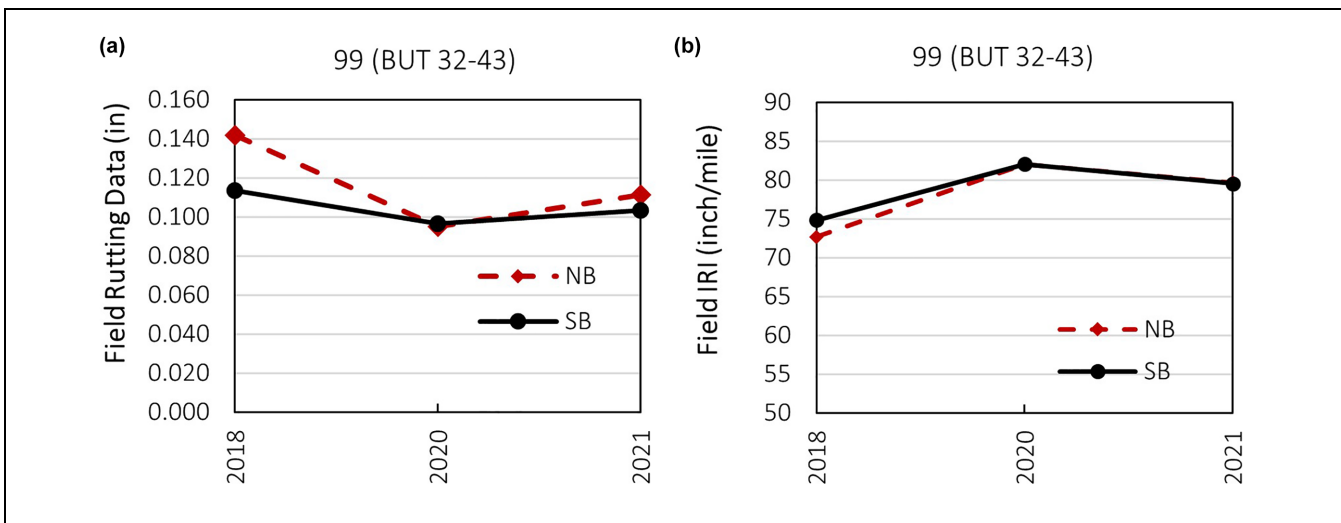


Figure 7. Field (a) rutting and (b) IRI data for 99 (BUT 32–43) NB and SB directions.
 Note: IRI = international rutting index; BUT = Butte County; NB = northbound; SB = southbound.

note that CalME models are calibrated to represent statewide median performance and, thus, are not expected to precisely match the performance of any specific project.

Highway 99 (BUT 32–43) Before and After Camp Fire. Figure 7, a and b, shows field rutting and IRI SB and NB of Highway 99 (BUT 32–43), with the NB having been used by the loaded trucks to clean up debris after Camp Fire. Field data indicated that the cracking of this highway was very close to zero during the period. Note that there were two lanes in each direction, and the data for the truck lane are shown here. According to

Table 4, the last structural treatment was carried out on this section in 2015, marking this section as 6 years old in 2021. The pavement exhibited 0.104 and 0.111 in. of rutting in each direction, with an IRI of 80 in./mi in both directions in 2021. This section was in “Good” condition in 2021 after fire debris removal meeting the federal criteria of 95 in./mi for IRI. The field data corroborated the previously illustrated pavement simulation results in Figures 3a and 4a, indicating an overall expected performance over the 20-year design life with no impact from the fire debris trucks.

With respect to visible trends in the physical conditions between the two directions, NB and SB showed

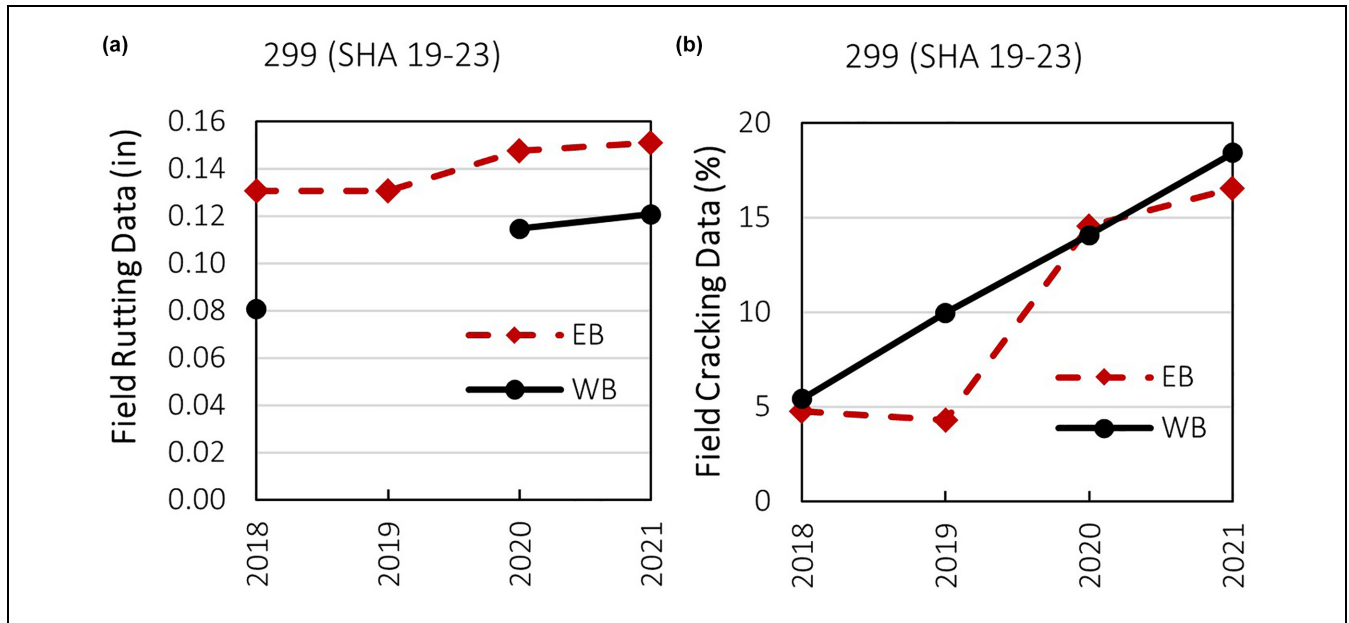


Figure 8. Field (a) rutting, and (b) cracking data for 299 (SHA 19–23) EB and WB directions.
 Note: IRI = international rutting index; SHA = Shasta County; EB = eastbound; WB = westbound.

similar changes of about a 10% increase in IRI from 2018 to 2020, indicating no significant debris removal. However, the reason for the drop in the field rutting data is unknown.

Highway 299 (SHA 19–23) Before and After Carr Fire. Figure 8, *a* to *c*, shows field rutting, cracking, and IRI data for the EB (used for debris removal) and westbound (WB) lanes of Highway 299 (SHA 19–23). Rutting and IRI data were unavailable for the WB lane in 2019. As seen in Table 3, the last structural treatment occurred in 2012, marking the pavement structure as 9 years old in 2021. The pavement section in the EB lane exhibited 0.151 in. of rutting, 16.5% fatigue cracking, and an IRI of 80 in./mi. The WB lane had less rutting at 0.121 in. but higher fatigue cracking at 18.4% and a higher IRI of 86 in./mi. Regardless of the variations between the distress and IRI in the two directions, the pavement section condition is classified as “Good” according to the federal IRI benchmark of 95 in./mi. Similarly, CalME simulations presented in Figure 4*a* predicted this section would perform well over the 20-year design life and would not incur impacts from debris trucks on this section’s rutting life or cracking.

In relation to any observable effects from Carr Fire debris removal in the field data, the rutting data comparison between 2018 and 2020 revealed a 13% increase in the EB lane, whereas the WB lane experienced a roughly 42% increase during the same period. However, data

were missing in 2019, so the precise increase during the debris removal is unknown. Consequently, the impact of the debris trucks is not clearly discernible in the rutting data for EB or may be obscured by other possible traffic growth inducing the accelerated damage in the WB direction during the same period as the Carr Fire debris removal. Conversely, based on cracking data (Figure 8*b*), the EB lane exhibited an increase from 4.3% in 2019 to 14.1% in 2020, which could be attributed to debris removal. CalME simulation results for this highway section (Figure 5*a*) did not suggest any impacts from fire debris removal.

Highway 191 (BUT 0–10) Before and After Carr Fire. Figure 9*a* shows the change in field cracking for Highway 191 (BUT 0–10), and Figure 9*b* presents the change in IRI for this section. According to Table 3, the last recorded structure of this section dates to 2013, indicating that the section was 8 years old in 2021. The cracking data showed a slightly higher cracking failure for the NB lane of this section, whereas the IRI results indicated that the increase in IRI for the SB lane was 12% higher than for the NB lane. The data suggest that the additional truck traffic from the fire did not significantly affect pavement cracking, which aligned with the simulation results illustrated in Figure 5*a*. Although the IRI results met the federal IRI benchmark of 95 in./mi, they also suggest that the debris removal traffic increased the roughness of the SB lane more than the NB lane.

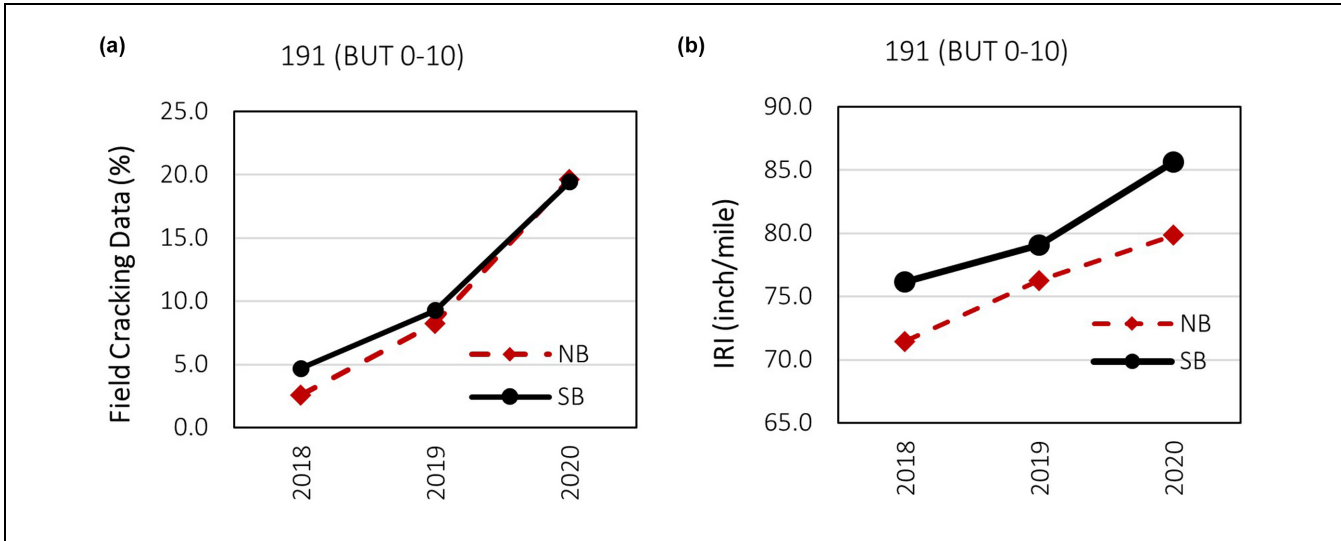


Figure 9. Field (a) cracking data and (b) IRI data for 191 (BUT 0–10) NB and SB directions.
 Note: IRI = international rutting index; BUT = Butte County; NB = northbound; SB = southbound.

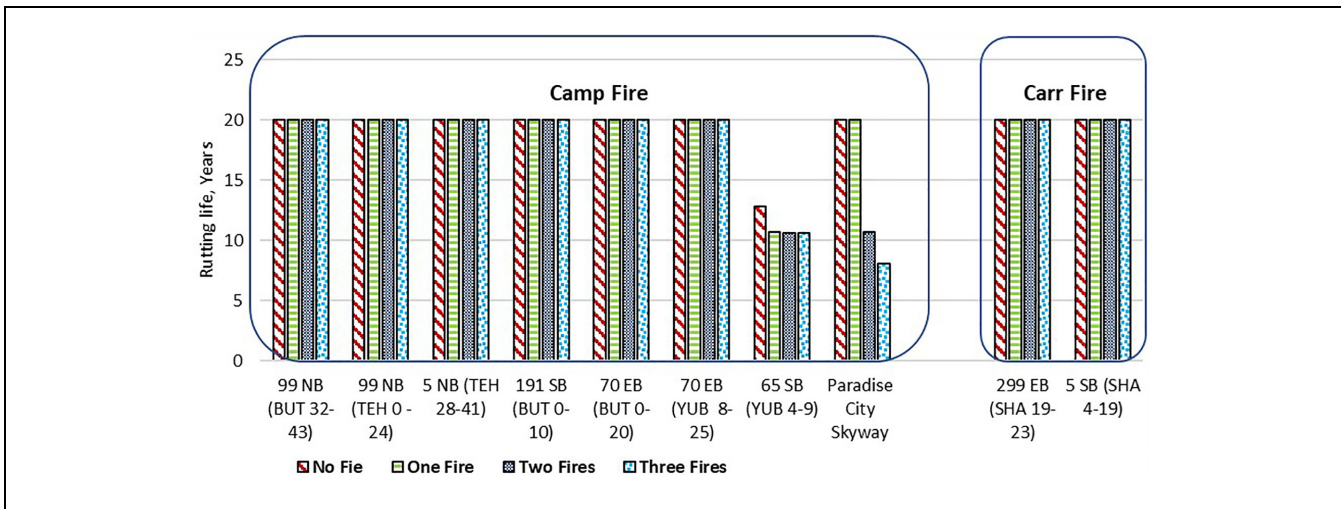


Figure 10. Impact of two- and three-times larger fires on the predicted rutting life.

This finding agrees with the simulation results shown in Figure 4b, which indicated that extra truck traffic increased the rutting depth in this section.

Sensitivity Analysis

Figures 10 and 11 present hypothetical scenarios in which the debris truckloads of the Camp or Carr Fires are twice and three times larger than the previously simulated pavements.

Based on the result shown in Figure 10, by multiplying the traffic generated by the Camp and Carr Fires by two and three, the rutting life of most of the simulated sections remained at least 20 years, whereas two sections

showed some changes. As mentioned, the high traffic volume for the structure of 65 SB (YUB 4–9) caused rutting failure in this section, which intensified with Camp Fire but did not change significantly with the hypothetical twice and thrice larger fires. The doubled and tripled traffic increased the TI by 0.11 and 0.11, respectively, compared with the TI from the actual fires.

In contrast, the doubled and tripled fires had a significant impact on the rutting life of Skyway, which was attributed to the significant increase in TI for this section (TI = 10.21 and 10.66 from the doubled and tripled fires, respectively) compared with the existing traffic (TI = 8.0).

As shown in Figure 11, similar to the actual fire, the doubled and tripled fires decreased the cracking life of 65

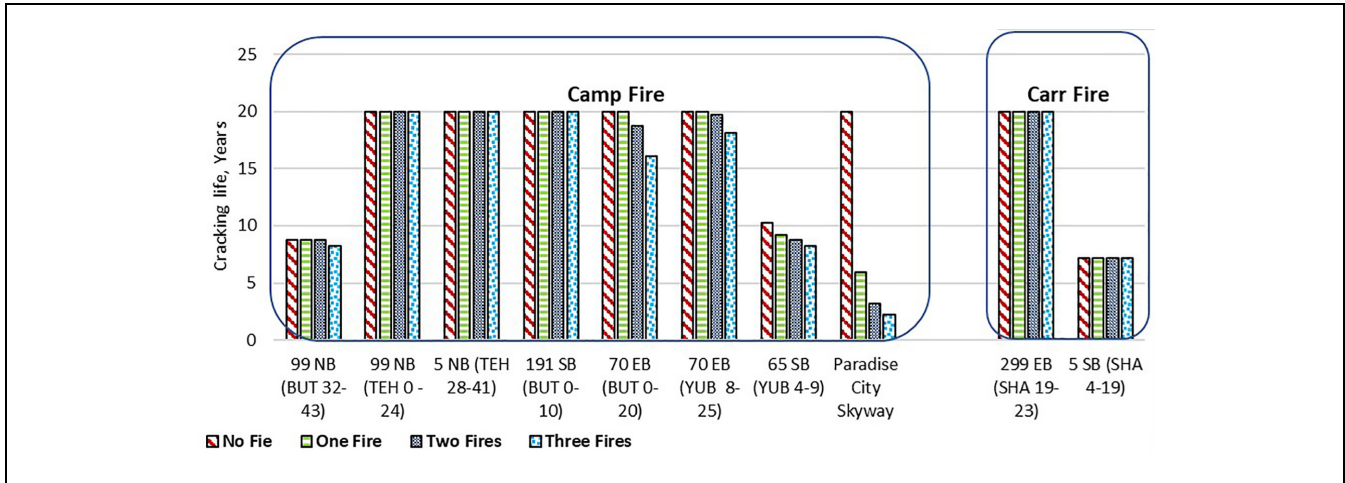


Figure 11. Impact of two- and three-times larger fires on the predicted fatigue cracking life.

SB (YUB 4-9) and Skyway, whereas they did not change the cracking life of 99 NB (TEH 0-24), 5 NB (TEH 28-41), 191 SB (BUT 0-10), 299 EB (SHA 19-23), or 5 SB (SHA 4-19) sections. However, owing to the higher traffic volumes generated by considering all three fires, the cracking life of the 99 NB (BUT 32-43), 70 EB (BUT 0-20), and 70 EB (YUB 8-25) sections decreased by 0.6, 3.9, and 17.8 years, respectively.

Conclusions

This study examined the structural state of highway pavement segments and a city street affected by debris transport to landfills and recycling facilities after two significant Northern California fire events in 2019—specifically, the Camp Fire and Carr Fire. Nine highway sections and one major city street were included in the study. Pavement structural design simulations were used to determine the impact of debris truck loads and volumes on pavement rutting and cracking lives.

The results of the pavement simulations showed that the structures that were not strong enough, notably Highway 65 (YUB 4-9), with a relatively thin HMA layer and AB layer, showed signs of early fatigue cracking failure. Because of the inadequate structural capacity, the slight increase in TI for this highway section led to a reduction of cracking life by almost 1 year and rutting by less than 1 year. Conversely, highways 99 NB (TEH 0-24), I-5 northbound and southbound, 191 SB, 70 EB, and 299 EB showed no signs of premature failure as a result of the additional truck traffic. One conclusion from the simulated pavement sections is that vulnerable pavements could be identified during the traffic planning phase as those not having sufficient structure to withstand their existing traffic.

A major city street in Paradise, Skyway, carried the majority of trucks hauling debris to all facilities. The increase of 1.53 in TI significantly affected this pavement’s fatigue cracking life, showing almost a 75% reduction in cracking life and a 0.19-in. increase in rutting.

In the case of the Carr Fire, which was smaller than Camp Fire and generated 14% of the debris of Camp Fire, the additional truck traffic did not affect the pavement life of the highways in Shasta County.

The sensitivity analysis of increasing the intensity of fire events to generate double or triple the amount of debris truck traffic as the Camp and Carr Fires showed a significant impact on the pavement structural life, especially the cracking life. The impact was induced on those pavement sections that were not affected by Camp Fire or Carr Fire events, such as Highway 70 EB (BUT 0-7).

Analysis of the limited available field data for three of the simulated highway sections showed that, despite some variations between simulation results and field data, the two studied sections used for the Camp Fire cleanup demonstrated satisfactory performance after Camp Fire. Furthermore, Highway 299, used for the Carr Fire cleanup, showed a 10% increase in fatigue cracking in the debris removal period but generally maintained a “Good” status based on IRI criteria alone. These findings indicate that budgets should be allocated to enable highway agencies to perform structural testing such as falling weight deflection testing in addition to pavement condition assessment before and closely after cleanup operations so the exact impact of the cleanup operation can be more precisely quantified for future planning.

The study concludes that wildfires could affect pavement life, especially fatigue cracking; however, the extent of the damage will depend on the amount of fire debris

remaining after the event, which will determine the additional truck traffic volumes and axle loads. The case studies presented here could be extended to include pavement simulations for other fire incidents to arrive at broader, network-level conclusions that state agencies and local governments could use for resilient planning. Furthermore, vulnerable highway sections could be identified and avoided as part of traffic planning during debris management operations. Based on the case studies, HMA thickness and TI values were identified as influential factors.

Acknowledgments

Jessica Erdahl and Marc Mattox from the Public Works Department of the City of Paradise are greatly appreciated for sharing the information necessary for the study. Timothy Roberts, Forest Health, Wood Products and Bioenergy at Cal Fire are thanked for sharing information. Todd Thalhamer, Chris McSwain, and other individuals of CalRecycle are thanked for assisting with sourcing the environmental reports for each fire event. Imad Basheer and Shahna Thomas of Caltrans are also thanked for their support of the study.

Author Contributions

The authors confirm contribution to the paper as follows: study conception and design: S. Nassiri, AA Butt; data collection: AA Butt, C. Kim, A. Zarei, S. Nassiri, J. Erdahl; analysis and interpretation of results: A. Zarei, C. Kim, AA Butt, S. Nassiri; draft manuscript preparation: AA Butt, C. Kim, A. Zarei, S. Nassiri, R. Wu, J. Erdahl, J.D. Lea. All authors reviewed the results and approved the final version of the manuscript.





Declaration of Conflicting Interests

The authors declared no potential conflicts of interest with respect to the research, authorship, and/or publication of this article.

Funding

The authors disclosed receipt of the following financial support for the research, authorship, and/or publication of this article: This study was made possible through funding received by the University of California Institute of Transportation Studies from the State of California via the Public Transportation Account and the Road Repair and Accountability Act of 2017 (SB 1).

ORCID iDs

Ali Zarei  <https://orcid.org/0000-0002-0729-3905>
 Changmo Kim  <https://orcid.org/0000-0001-9652-8675>
 Ali Azhar Butt  <https://orcid.org/0000-0002-4270-8993>
 Rongzong Wu  <https://orcid.org/0000-0001-7364-7583>
 Jeremy David Lea  <https://orcid.org/0000-0003-3445-8661>
 Somayeh Nassiri  <https://orcid.org/0000-0001-5367-2167>

References

1. Conservation Biology Institute, and The Nature Conservancy. Paradise Nature-Based Fire Resilience Project. Paradise Recreation & Park District, 2020. <https://consbio.org/reports/paradise-nature-based-fire-resilience-project/>.
2. Radeloff, V. C., D. P. Helmers, H. A. Kramer, M. H. Mockrin, P. M. Alexandre, A. Bar-Massada, V. Butsic, et al. Rapid Growth of the US Wildland-Urban Interface Raises Wildfire Risk. *Proceedings of the National Academy of Sciences*, Vol. 115, 2018, pp. 3314–3319. <https://doi.org/10.1073/pnas.1718850115>.
3. Zurich North America. *California Fires: Building Resilience from the Ashes*. Zurich American Insurance Company, Schaumburg, IL, 2019.
4. Fraser, A. M., M. V. Chester, and B. S. Underwood. Wildfire Risk, Post-Fire Debris Flows, and Transportation Infrastructure Vulnerability. *Sustainable and Resilient Infrastructure*, Vol. 7, No. 3, 2022, pp. 188–200. <https://doi.org/10.1080/23789689.2020.1737785>.
5. Caltrans. *California Test 382-Determination of Asphalt Content of Bituminous Mixtures by the Ignition Method*. 2001. <https://dot.ca.gov/-/media/dot-media/programs/engineering/documents/californiatestmethods-ctm/ctm-382-jun-2001-a11y.pdf>
6. Peker, M. A. Evaluation of Concrete Pavers Affected by Manavgat Wildfires. *Journal of Sustainable Construction Materials and Technologies*, Vol. 6, No. 4, 2021, pp. 168–172. <https://doi.org/10.14744/jscmt.2021.05>.
7. Sancak, E., Y. Dursun Sari, and O. Simsek. Effects of Elevated Temperature on Compressive Strength and Weight Loss of the Light-Weight Concrete with Silica Fume and Superplasticizer. *Cement and Concrete Composites*, Vol. 30, No. 8, 2008, pp. 715–721. <https://doi.org/10.1016/j.cemconcomp.2008.01.004>.
8. Daware, A., A. B. Peerzada, M. Z. Naser, P. Rangaraju, and B. Butman. Examining the Behavior of Concrete Masonry Units Under Fire and Post-fire Conditions. *Fire and Materials*, Vol. 47, No. 2, 2023, pp. 159–169. <https://doi.org/10.1002/fam.3085>.
9. Khoury, G. A. Effect of Fire on Concrete and Concrete Structures. *Progress in Structural Engineering and Materials*, Vol. 2, No. 4, 2000, pp. 429–447. <https://doi.org/10.1002/pse.51>.
10. Rengers, F. K., L. A. McGuire, N. S. Oakley, J. W. Kean, D. M. Staley, and H. Tang. Landslides After Wildfire: Initiation, Magnitude, and Mobility. *Landslides*, Vol. 17, No. 11, 2020, pp. 2631–2641. <https://doi.org/10.1007/s10346-020-01506-3>.
11. Domingo, N., and H. Luo. Canterbury Earthquake Construction and Demolition Waste Management: Issues and Improvement Suggestions. *International Journal of Disaster Risk Reduction*, Vol. 22, 2017, pp. 130–138. <https://doi.org/10.1016/j.ijdrr.2017.03.003>.
12. Karunasena, G., and D. Amaratunga. Capacity Building for Post Disaster Construction and Demolition Waste Management: A Case of Sri Lanka. *Disaster Prevention and Management*, Vol. 25, No. 2, 2016, pp. 137–153. <https://doi.org/10.1108/DPM-09-2014-0172>.

13. MacArthur, J., P. Mote, M. A. Figliozzi, J. Ideker, and M. Lee. *Climate Change Impact Assessment for Surface Transportation in the Pacific Northwest and Alaska*. Portland State University Library. Transportation Research and Education Center (TREC), Portland, OR, 2012.
14. Constant Associates. After Action Report. Town of Paradise. https://www.catf3.org/after-action-reports#h.p_-o5SPIPXU9MZ
15. Cal Fire. Camp Fire. <https://www.fire.ca.gov/incidents/2018/11/8/camp-fire/>. Accessed July 2, 2023.
16. Hamideh, S., P. Sen, and E. Fischer. Wildfire Impacts on Education and Healthcare: Paradise, California, After the Camp Fire. *Natural Hazards*, Vol. 111, No. 1, 2022, pp. 353–387. <https://doi.org/10.1007/s11069-021-05057-1>.
17. Tetra Tech Inc. *Camp Fire Incident Butte County, California Final Summary Report*. California Department of Resources, Recycling, and Recovery, Sacramento, CA, 2020.
18. East, A. E., J. B. Logan, P. Dartnell, O. Lieber-Kotz, D. B. Cavagnaro, S. W. McCoy, and D. N. Lindsay. Watershed Sediment Yield Following the 2018 Carr Fire, Whiskeytown National Recreation Area, Northern California. *Earth and Space Science*, Vol. 8, No. 9, 2021, e2021EA001828. <https://doi.org/10.1029/2021EA001828>.
19. CalFire. Carr Fire. CAL FIRE. <https://www.fire.ca.gov/incidents/2018/7/23/carr-fire>. Accessed July 31, 2023.
20. Whiskeytown. National Park Service Releases Investigation Report for 2018 Carr Fire. Whiskeytown National Recreation Area (U.S. National Park Service). <https://www.nps.gov/whis/learn/news/national-park-service-releases-investigation-report-for-2018-carr-fire.htm>. Accessed July 31, 2023.
21. Schmidt, J. Vegetation Cover and Structure Loss in Four Northern California Wildfires: Butte, Tubbs, Carr, and Camp. <https://mpr.ub.uni-muenchen.de/104232/>. Accessed May 30, 2022.
22. Tetra Tech, Inc. *Carr Fire Incident Shasta County, California Final Environmental Report*. California Department of Resources, Recycling, and Recovery CalRecycle Engineering Support Unit, Sacramento, CA, 2020.
23. State of California, Department of Transportation, and California Highway Patrol, and California Department of Resources Recycling and Recovery. *Camp Fire Debris Removal Operation Traffic Management Plan*. Transportation Management Evaluation Camp Fire Debris Removal Operations, Sacramento, CA, 2019.
24. Caltrans. Traffic Census Program. Caltrans. <https://dot.ca.gov/programs/traffic-operations/census>. Accessed August 1, 2023.
25. Caltrans. Pavement Management. Caltrans. <https://dot.ca.gov/programs/maintenance/pavement/pavement-management>. Accessed August 1, 2023.
26. Kim, C., J. D. Lea, V. Kannekanti, and J. T. Harvey. Updating Weigh-in-Motion (WIM) Spectra in Pavem. University of California Pavement Research Center, UC Davis, 2022. <https://doi.org/10.7922/G2JD4V3M>.
27. Nassiri, S., A. A. Butt, A. Zarei, C. Kim, R. Wu, J. D. Lea, and J. Erdahl. Evaluating Road Resilience to Wildfires: Case Studies of Camp and Carr Fires. *The University of California Institute of Transportation Studies*, 2023. <https://doi.org/10.7922/G2DJ5D0D>.
28. Deacon, J. A., J. T. Harvey, I. Guada, L. Popescu, and C. L. Monismith. Analytically Based Approach to Rutting Prediction. *Transportation Research Record: Journal of the Transportation Research Board*, 2002. 1806: 9–18.
29. Wu, R., J. Harvey, J. Lea, A. Mateos, S. Yang, and N. Hernandez. Updates to CalME and Calibration of Cracking Models. University of California Pavement Research Center, UC Davis, 2021. <https://doi.org/10.7922/G2CR5RNT>.
30. Wu, R., J. Zhou, and J. T. Harvey. Development of the CalME Standard Materials Library. University of California Pavement Research Center, UC Davis, 2018.
31. University of California Pavement Research Center. iGPR. <http://www.ucprc.ucdavis.edu/PaveM-Portal/>. Accessed July 31, 2023.
32. California Department of Transportation (Caltrans). Maintenance Manual. Caltrans. <https://dot.ca.gov/programs/maintenance/maintenance-manual>. Accessed August 1, 2023.
33. California Department of Transportation (Caltrans). 2020 State of the Pavement Report. 2020. https://dot.ca.gov/-/media/dot-media/programs/maintenance/documents/office-of-pavement-management/sop/2020_sop_report-a11y-v2.pdf